Supporting Information

Natural Ginkgo Tree Leaves as Piezo-Energy Harvesters

Dingyun Shao ⊥, Chuanfeng Wang ⊥, Wei Li, Liang Lu, Jun Lu #, *, Weiqing Yang *

Key Laboratory of Advanced Technologies of Materials, Ministry of Education, School of Materials Science and Engineering, Southwest Jiaotong University, Chengdu 610031, Sichuan, China

---

⊥ These authors equally contributed to this work.

Other used names Jun Lv and Jun Lyu.

* Corresponding authors. E-mail: junluprc@hotmail.com (J. Lu), wqyang@swjtu.edu.cn (W.Q. Yang).

Experimental Section

Materials and Reagents: Yellow ginkgo tree leaves were collected from the campus of Southwest Jiaotong University, Chengdu, China. Blue silica gel particles were supplied by Shengda Desiccant Co., Ltd, Suzhou, China. The fresh ginkgo leaves were cleaned with distilled water. Then they were buried in the blue silica gel particles for 36 h. Thereafter, the dried ginkgo leaves were removed from the silica gel desiccant. Without any further chemical treatment, they were used directly for the device fabrication.

Characterization of Materials: Field emission scanning electron microscopy (FE-SEM) was conducted on a FEI Inspect F apparatus. Polarized optical microscopy (POM) was performed using a YJ-2005BP microscope for low magnification imaging and then using a DM2700P microscope for high magnification imaging. Attenuated total reflectance Fourier transform infrared (ATR-FTIR) spectra were obtained using a Nicolet iS20 spectrometer. X-ray diffraction (XRD) data were acquired on a PANalytical X'pert PRO diffractometer. Pole figures were measured using a PANalytical Empyrean Series 2 X-ray diffraction system. The polar angle α ranged from 0^{o} to 60^{o}, and the azimuthal angle β ranged from 0^{o} to 360^{o}, with a step size of 5^{o} for both α and β. The incomplete pole figures were used as the input for orientation distribution function (ODF) analysis using MTEX opensource package [1-3]. The complete pole figures were then recomputed from the ODF results. The ferroelectric and piezoelectric properties of unpoled ginkgo tree leaf were measured using a TF Analyzer 2000E instrument.

Fabrication of PENGs: The piezoelectric nanogenerator (PENG) was prepared from intact, dried natural ginkgo leaf, aluminum (Al) electrodes, and polyurethane tape (PU), in a sandwich structure, as shown in Figure 3a. First, two layers of aluminum films were attached to the top and bottom sides of a ginkgo leaf. They were used as electrodes to derive piezoelectric signals. Next, the Al electrodes were encapsulated using PU tape. Finally, the PENG device was fixed to the acrylic (PMMA) plates to ensure a smooth shock during the subsequent piezoelectric measurement. The impact head of measurement system was also made of the same acrylic resin to eliminate possible interference from triboelectric charges. The prepared ginkgo leaf based piezoelectric nanogenerator (GL-PENG) has an area of 20 mm×20 mm and a thickness of 0.125 mm, as shown in Figure 3b.

Test of Devices: The piezoelectric performance of natural ginkgo leaf was further evaluated by measuring the electrical outputs of the GL-PENG device under dynamic impulse forces (Figure 3e). The NTIAG HS01-37×166 linear motor was used as the impulse source. The output voltage signals were collected using a Keithley 6514 system electrostatic meter. The output current signals were measured using a Stanford Research SR570 low noise current amplifier. The transferred charge was calculated by integrating the positive or the negative current peak over one cycle [4, 5]. The output voltage signals of human coughing and human speech were collected using a Keithley DAQ6510 oscilloscope. Switching polarity test was also performed on the natural ginkgo leaf based PENG device (Figure 3f). The wave patterns were in the opposite directions for the forward- and reverse-connected circuits. This clearly validated the output electrical signals come directly from the piezoelectric responses of the GL-PENG, rather than from the influence of measurement system or environment [6, 7].

Monitoring of Human Physiology: The relevant biological signals involved in this article were collected from the volunteers. The informed consent was obtained prior to the research. The relevant experiments involving human subjects conformed to the local ethical requirements.

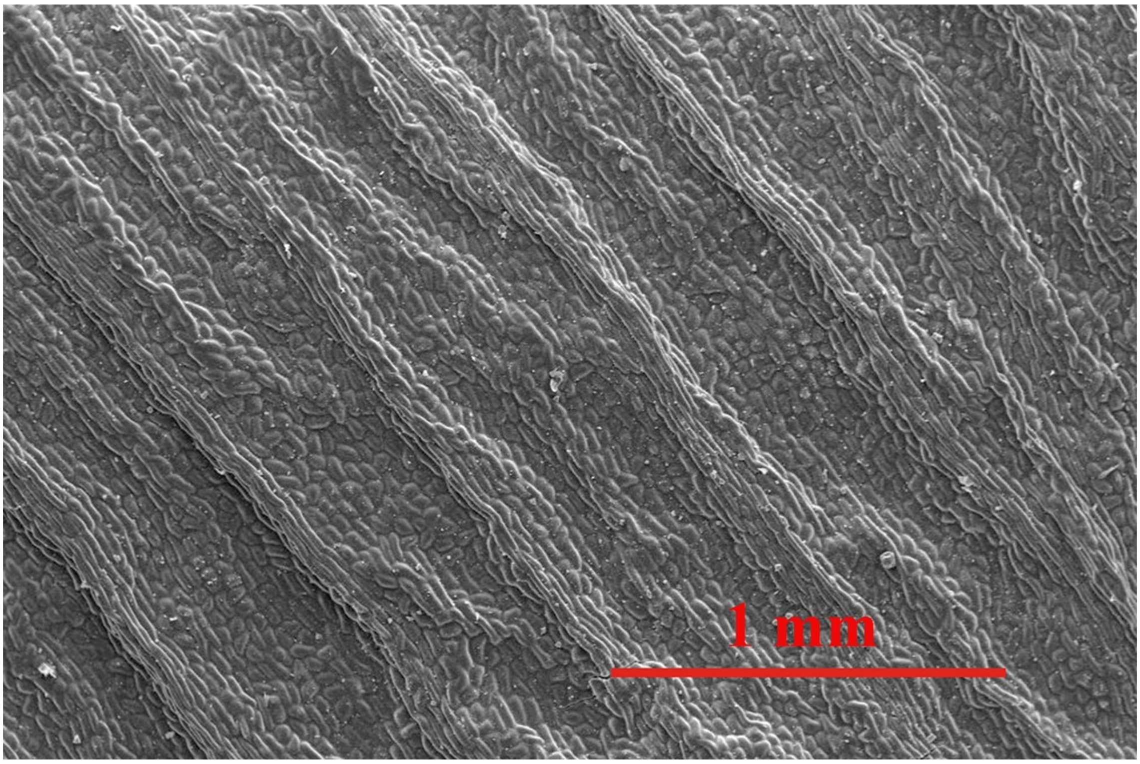

Figure S1. Typical FE-SEM image of the surface of a natural ginkgo tree leaf.

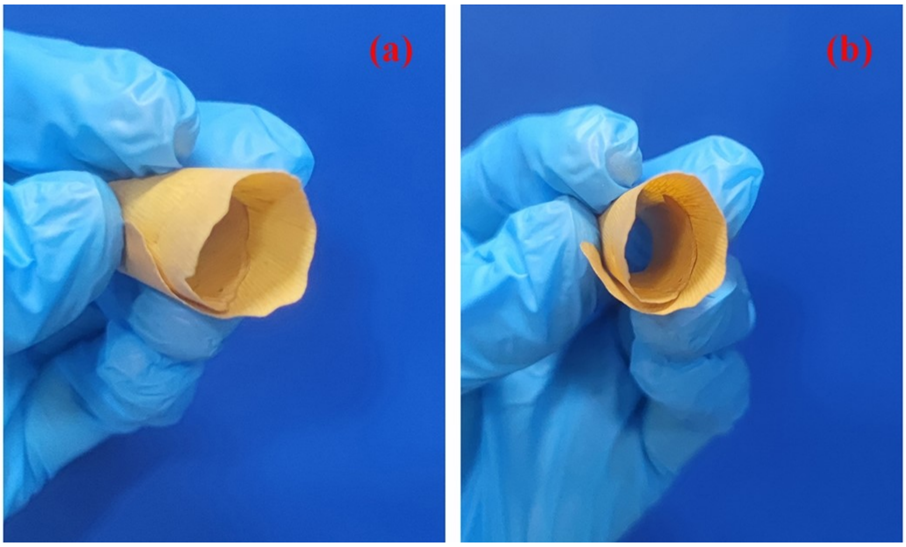

Figure S2. Demonstration of good flexibility of natural ginkgo tree leaves in the rolling-up mode. The yellow ginkgo tree leaves were buried in blue silica gel particles and physically dried for 36 h.

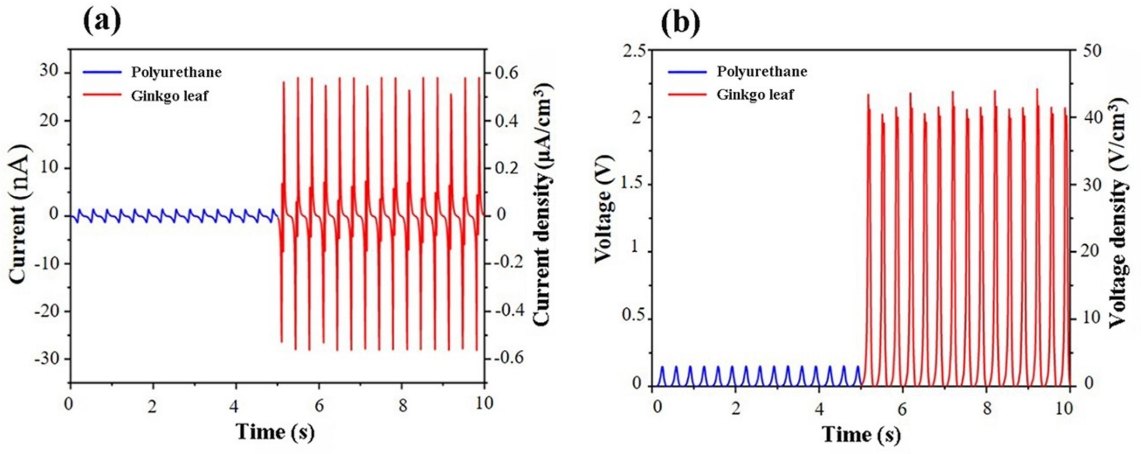

Figure S3. A comparison of a) short-circuit current outputs and b) open-circuit voltage outputs of piezoelectric ginkgo leaf (GL) and non-piezoelectric polyurethane (PU) tape, respectively. Aluminum (Al) foil was used as electrode material for both types of sandwich structured devices. The Al:GL:Al trilayer square and the Al:PU:Al trilayer square were further encapsulated using PU tape for device-level testing, respectively. The devices were stimulated using a 8-N and 3-Hz impulse force. Device area: 20 mm×20 mm.

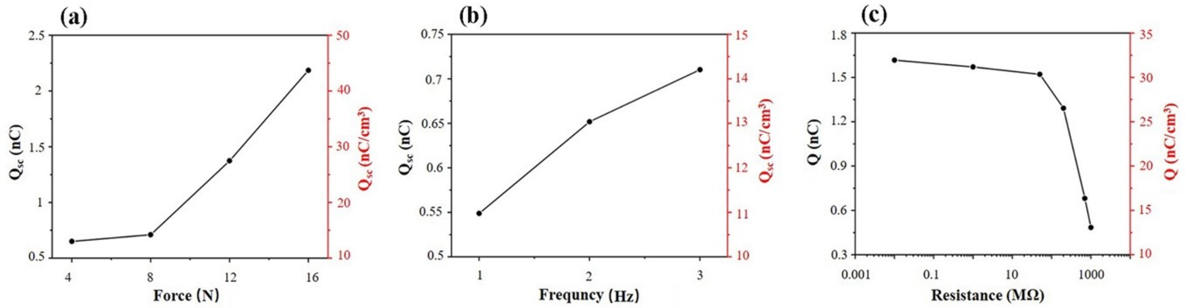

Figure S4. Transferred charge of ginkgo-leaf device. a) Dependence on force amplitude, measured at a fixed frequency of 3.0 Hz. b) Dependence on force frequency, measured at a fixed amplitude of 8 N. c) Dependence on load resistance, measured under a 16-N and 3-Hz impulse force. The transferred charge is proportional to a) force amplitude, and b) force frequency, while inversely proportional to c) load resistance. Device size: 20 mm×20 mm in area and 0.125 mm in thickness.

Table S1. A comparison of the measured ferroelectric response of ginkgo tree leaf with the reported nature-driven bioorganic ferroelectric materials.

Material	Source	Treatment	Remnant polarization (P_r) ($\mu C\ cm^{-2}$)	Coercive field (E_c) ($kV\ cm^{-1}$)	Piezoelectric coefficient (d_{33})	Ref.
Fish scale	Animal	Unpoled	0.29	100	-5 $pC\ N^{-1}$	[8]
Fish swim bladder	Animal	Unpoled	1.1	15	22 $pC\ N^{-1}$	[9]
Fish skin	Animal	Unpoled	0.12	22	-3 $pC\ N^{-1}$	[10]
Prawn shell	Animal	Unpoled	0.14	20	-2 $pC\ N^{-1}$	[11]
Spider silk	Animal	Unpoled	0.45	NF	0.36 $pm\ V^{-1}$	[12]
Squid pen β-chitin	Animal	Unpoled	NF	NF	3.986 $pm\ V^{-1}$	[13]
Aloe vera	Plant	Poled	0.61	24	6.5 $pm\ V^{-1}$	[14]
Onion skin	Plant	Unpoled	0.053	10-15	2.8 $pC\ N^{-1}$	[15]
Pomelo fruit membrane	Plant	Unpoled	0.027	6-8	4.6 $pC\ N^{-1}$	[16]
Tomato peel	Plant	Unpoled	12.76×10^{-5}	NF	NF	[17]
Ginkgo tree leaf	**Plant**	**Unpoled**	**0.12**	**20**	**6.44 $pm\ V^{-1}$**	**Present work**

Table S2. A comparison of the piezoelectric output of ginkgo-leaf device with the recently reported bioorganic materials based piezoelectric nanogenerators.

Material	Device area (mm^2)	Piezoactive layer thickness (μm)	Voltage/ Current	Charge	Voltage density [a] ($V\ cm^{-3}$)	Current density [a] ($\mu A\ cm^{-3}$)	Charge density [a] ($nC\ cm^{-3}$)	Ref.
Ginkgo tree leaf	**20 × 20**	**125**	**6.55 V/ 125 nA**	**2.18 nC**	**131**	**2.5**	**43.7**	**Present work**
Fish scale	NF	250	4 V/ 1.5 μA	213 pC	_	_	_	[8]
Fish swim bladder	17.5 × 13.5	253	10 V/ 51 nA	NF	167	0.85	_	[9]
Prawn shell	12.95 × 7.37	130	1 V/ 1 nA	0.3 pC	81	0.081	2.4×10^{-2}	[11]
Squid pen β-chitin	60 × 100	35	1.04 V/ 177 $nA\ cm^{-2}$	NF	4.95	50.57	_	[13]
Aloe vera	40 × 40	27	1.19 V/ 547 nA	NF	27.55	12.66	_	[14]
Onion skin	30 × 20	240	18 V/ 166 nA	48 pC	125	1.2	3.3×10^{-1}	[15]
Tomato peel	40 × 60	NF	1.02 $V\ cm^{-2}$/ 104 $nA\ cm^{-2}$ [a]	NF	_	_	_	[17]
Peptide	12 × 12	NF	0.6 V/ 7 nA	NF	_	_	_	[18]
Polylactide	20 × 20	320	9.5 V/ 620 nA	NF	74.2	4.9	_	[19]
Chitosan	10 × 10	200	2.5 V/ 30 nA	NF	125	1.5	_	[20]

[a] Values calculated based on other parameters reported in the references.

References

[1] R. Hielscher and H. Schaeben, *J. Appl. Crystallogr.*, 2008, **41**, 1024-1037.

[2] F. Bachmann, R. Hielscher and H. Schaeben, *Solid State Phenom.*, 2010, **160**, 63-68.

[3] X. J. Wu, L. Pu, Y. F. Xu, J. C. Shi, X. Y. Liu, Z. Y. Zhong and S. N. Luo, *RSC Adv.*, 2018, **8**, 22583-22591.

[4] N. Wu, X. Cheng, Q. Zhong, J. Zhong, W. Li, B. Wang, B. Hu and J. Zhou, *Adv. Funct. Mater.*, 2015, **25**, 4788-4794.

[5] H. Wu, Z. F. Chen, G. Q. Xu, J. B. Xu, Z. K. Wang and Y. L. Zi, *ACS Appl. Mater. Interfaces*, 2020, **12**, 56060-56067.

[6] Y. S. Yang, Y. Qin, C. Li, L. M. Dai and Z. L. Wang, *Appl. Phys. Lett.*, 2009, **94**, 022905.

[7] S. Y. Ma, L. Jin, X. Huang, C. Riziotis, R. Huang, C. L. Zhang, J. Lu and W. Q. Yang, *Adv. Mater. Interfaces*, 2018, **5**, 1800587.

[8] S. K. Ghosh and D. Mandal, *Appl. Phys. Lett.*, 2016, **109**, 103701.

[9] S. K. Ghosh and D. Mandal, *Nano Energy*, 2016, **28**, 356-365.

[10] S. K. Ghosh and D. Mandal, *ACS Sustainable Chem. Eng.*, 2017, **5**, 8836-8843.

[11] S. K. Ghosh and D. Mandal, *Appl. Phys. Lett.*, 2017, **110**, 123701.

[12] S. K. Karan, S. Maiti, O. Kwon, S. Paria, A. Maitra, S. K. Si, Y. Kim, J. K. Kim and B. B. Khatua, *Nano Energy*, 2018, **49**, 655-666.

[13] K. Kim, M. Ha, B. Choi, S. H. Joo, H. S. Kang, J. H. Park, B. Gu, C. Park, C. Park, J. Kim, S. K. Kwak, H. Ko, J. Jin and S. J. Kang, *Nano Energy*, 2018, **48**, 275-283.

[14] N. R. Alluri, N. P. M. J. Raj, G. Khandelwal, V. Vivekananthan and S. J. Kim, *Nano Energy*, 2020, **73**, 104767.

[15] S. Maiti, S. K. Karan, J. Lee, A. K. Mishra, B. B. Khatua and J. K. Kim, *Nano Energy*, 2017, **42**, 282-293.

[16] S. Bairagi, S. Ghosh and S. W. Ali, *Sci. Rep. – UK*, 2020, **10**, 12121.

[17] Q. M. Saqib, M. U. Khan, H. Song, M. Y. Chougale, R. A. Shaukat, J. Kim, J. Bae, M. J. Choi, S. C. Kim, O. Kwon and A. Bermak, *Adv. Sustainable Syst.*, 2021, **5**, 2100066.

[18] K. Jenkins, S. Kelly, V. Nguyen, Y. Wu and R. Yang, *Nano Energy*, 2018, **51**, 317-323.

[19] Y. L. Xu, L. Jin, X. B. He, X. Huang, M. L. Xie, C. F. Wang, C. L. Zhang, W. Q. Yang, F. B. Meng and J. Lu, *J. Mater. Chem. A*, 2019, **7**, 1810-1823.

[20] W. Li, C. F. Wang, D. Y. Shao, L. Lu, J. J. Cao, X. L. Wang, J. Lu and W. Q. Yang, *Nanoscale*, 2022, **14**, 9031-9044.